

## Pyrimidine Derivatives as Corrosion Inhibitors for Carbon-Steel in 2M Hydrochloric Acid Solution

G.Y. Elewady

Chemistry Department, Faculty of Science, Mansoura University, Mansoura, Egypt

\*E-mail: [ghadaelewady@yahoo.com](mailto:ghadaelewady@yahoo.com)

Received: 24 June 2008 / Accepted: 29 July 2008 / Published: 8 September 2008

---

2,6-Dimethylpyrimidine-2-amine and two of its derivatives have been investigated as corrosion inhibitors for carbon-steel (C-steel) in 2M HCl solution using electrochemical impedance spectroscopy (EIS) and weight loss techniques. The efficiency of the inhibitors increases with increase in the inhibitor concentration. Results obtained reveal that the used pyrimidine derivatives perform as corrosion inhibitors for C-steel in 2M HCl. Double layer capacitance,  $C_{dl}$ , and charge transfer resistance,  $R_{ct}$ , values were derived from Nyquist and Bode plots obtained from A.C. impedance studies. Change in impedance parameters are indicative of the adsorption of these inhibitors on the iron surface. The inhibition efficiency mainly depends on the nature of the investigated compounds. The values of the inhibition efficiency calculated from the two techniques are in reasonably good agreement. The adsorption of these compounds on C-steel surface is found to obey Langmuir adsorption isotherm. The mechanism of inhibition was discussed in the light of the chemical structure of the undertaken inhibitors and their adsorption on C-steel surface.

---

**Keywords:** Corrosion inhibitors, C-steel, Electrochemical impedance spectroscopy, weight loss, HCl, pyrimidine derivatives.

### 1. INTRODUCTION

Hydrochloric acid is widely used for the removal of rust and scale in several industrial operations. The corrosion of carbon steel (C-steel) in such environments and its inhibition constitute a complex problem of process. The corrosion characteristics of steel in aggressive mineral acid media have been widely investigated (1-6). The corrosion of iron and its alloys and their inhibition by different organic inhibitors in acid solution has been studied by several authors (7-19). A perusal of the literature on acid corrosion inhibitors act by adsorption on the metal surface. This phenomenon could take place via (i) electrostatic attraction between the charged metal and the charged inhibitor molecules (ii) dipole-type interaction between uncharged electron pairs in the inhibitor with the metal, (iii)  $\pi$

electron-interaction with the metal, and (iv) a combination of all of the above (20). The compounds containing nitrogen can provide excellent inhibition in acid media.

The present investigation is concerned with the mechanism and efficiency of some pyrimidine derivatives as corrosion inhibitors of C-Steel in 2M HCl solution.

## 2. EXPERIMENTAL PART

### 2.1. Composition of material samples

The composition of C-steel specimens used in this work is

Element	C	Mn	P	Si	Fe
Weight (%)	0.2	0.35	0.024	0.003	Rest

### 2.2. Tested specimens and treatment

For weight loss measurements the C-steel were used in the form of sheets having a sample area of 5 cm<sup>2</sup>. Before the measurements, the samples were polished by 2/0 and 3/0 emery papers and cleaned in ultrasonic bath for 5 min., then decreased with acetone (21), washed with bidistilled water, and finally dried between two filter papers and weighed. The weighed samples are immersed in the corrosive medium for a certain period of time, then removed, washed with double distilled water, dried and weighed again. The percentage inhibition efficiency (%IE) and the surface coverage ( $\theta$ ) were computed from the following equations

$$\%IE = \left( 1 - \frac{W_{\text{add}}}{W_{\text{free}}} \right) \times 100 \quad (1)$$

$$\theta = \left( 1 - \frac{W_{\text{add}}}{W_{\text{free}}} \right) \quad (2)$$

where  $w_{\text{free}}$  and  $w_{\text{add}}$  are the weight loss in corrosive medium and in inhibited solution in mg cm<sup>-2</sup> respectively.

For electrochemical impedance spectroscopy (EIS) measurements polishing and cleaning of C-steel electrodes were carried out in a similar way to that used in the case of weight loss measurements. The electrodes used were cut from wire of a diameter 0.6 mm. Then fixed with epoxy resin at one end into a Pyrex glass tubing of appropriate diameter leaving the exposed length, 1 cm, to contact the solution. The EIS measurements were carried out in a conventional three-electrode glass cell with a platinum counter electrode and a saturated calomel electrode (SCE) as a reference electrode. C-steel rod is the working electrode. The cell was kept at a constant temperature (25±0.1°C).

From EIS data, the percentage inhibition efficiency (%IE) and the surface coverage ( $\theta$ ) were calculated from the following equations

$$\%IE = \left(1 - \frac{R_{cto}}{R_{ct}}\right) \times 100 \quad (3)$$

$$\theta = \left(1 - \frac{R_{cto}}{R_{ct}}\right) \quad (4)$$

where  $R_{cto}$  and  $R_{ct}$  are the charge transfer resistance in the absence and presence of inhibitor respectively.

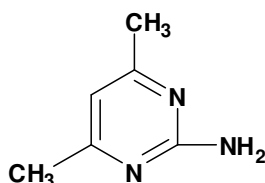
### 2.3. Apparatus

EIS measurements were carried out using as signals (10 mV) peak to peak at the open circuit potential in the frequency range 100 KHz – 10 mHz. Time interval of 15 min was given for steady state attainment of open circuit potential then, the A.C. impedance measurements were carried out. The impedance of the electrochemical system was measured using 1M be system (Zahner Elektrik, Germany) with impedance measurement unit. Impedance data through this work were represented by a simple equivalent circuit model which is equivalent to the well-known Randles Cell (22).

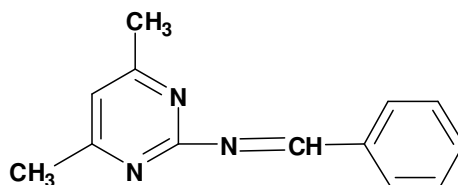
### 2.4. Materials and solutions

Hydrochloric acid solution was prepared from chemically pure grade (BDH) by appropriate dilution, and then standardized using sodium carbonate. Double distilled water was used through out all experiments.

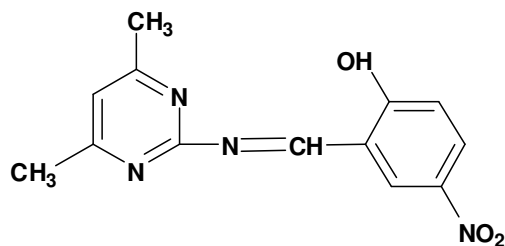
The synthesis and characterization (IR spectra and elemental analysis) of the pyrimidine compounds were as described and documented previously (23). Structural formulae of the inhibitors examined are shown below.



Inhibitor I: 4,6-Dimethylpyrimidine-2-amine



Inhibitor II: N-Benzylidene-4,6-dimethylpyrimidine-2-amine



Inhibitor III: 2-[(3,6-Dimethylpyridimino-2-ylimino)methyl]-4-nitrophenol

### 3. RESULTS AND DISCUSSION

#### 3.1. Electrochemical Impedance Spectroscopy (EIS)

The corrosion behavior of C-steel in 2M HCl solution in the presence of the pyrimidine derivatives was investigated by the EIS method at 25°C. The Nyquist and Bode plots are shown in Figures (1-6). For Nyquist plots (Figures 1-3) it is clear that the impedance diagrams in most cases does not show perfect semicircle. This behavior can be attributed to the frequency dispersion (24) as a result of roughness and in homogenates of the electrode surface. The impedance response consisted of characteristic semicircles for solutions examined indicating that the dissolutions of C-steel process occurs under charge transfer control in other words under activation control and the presence of the inhibitors does not change the mechanism of the acid dissolution. These semicircles are of a capacitive type whose diameters increase with increasing inhibitor concentration.

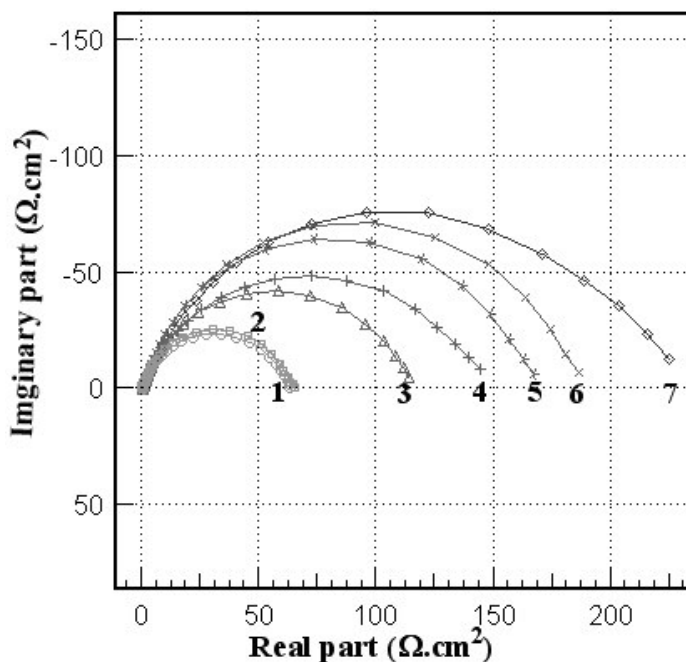


**Figure 1.** Nyquist plots of C-steel in 2M HCl in presence of different concentrations of inhibitor I at 25 °C. (1) blank, (2)  $1 \times 10^{-5}$  M, (3)  $5 \times 10^{-5}$  M, (4)  $1 \times 10^{-4}$  M, (5)  $5 \times 10^{-4}$  M, (6)  $1 \times 10^{-3}$  M and (7)  $5 \times 10^{-3}$  M

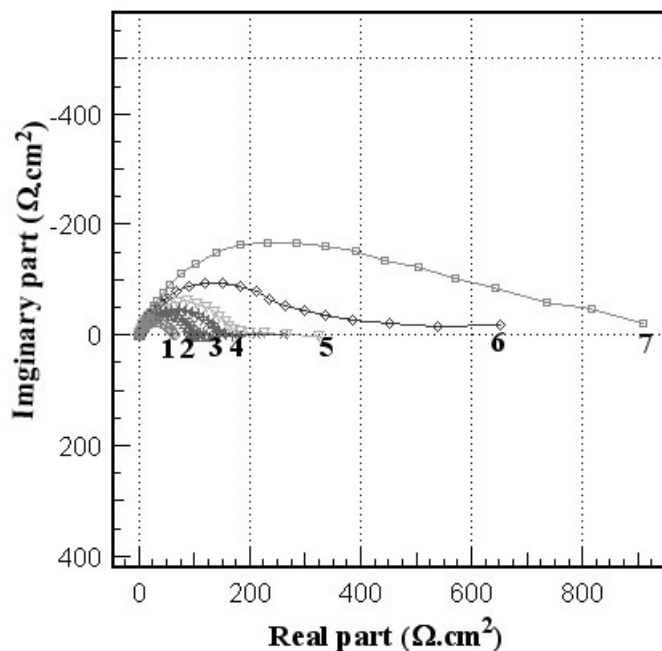


**Figure 2.** Nyquist plots of C-steel in 2M HCl in presence of different concentrations of inhibitor II at 25 °C. (1) blank, (2)  $1 \times 10^{-5}$  M, (3)  $5 \times 10^{-5}$  M, (4)  $1 \times 10^{-4}$  M, (5)  $5 \times 10^{-4}$  M, (6)  $1 \times 10^{-3}$  M and (7)  $5 \times 10^{-3}$  M

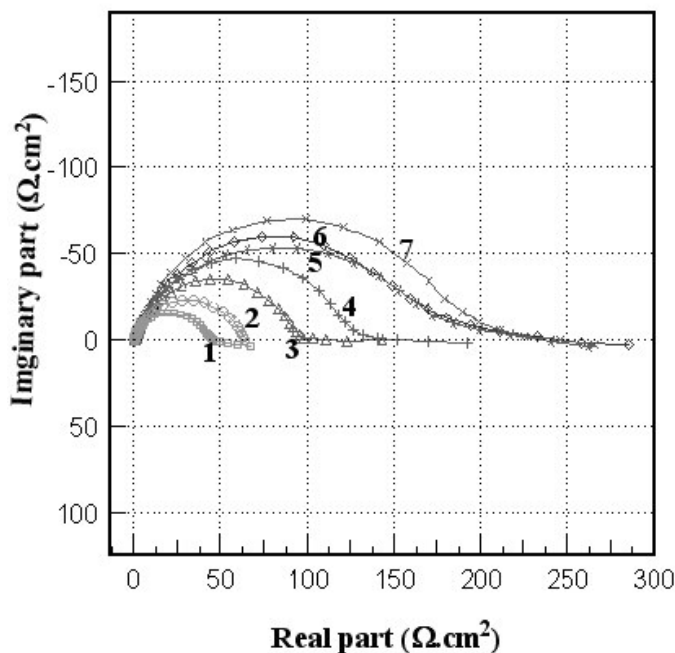


**Figure 3.** Nyquist plots of C-steel in 2M HCl in presence of different concentrations of inhibitor III at 25 °C. (1) blank, (2)  $1 \times 10^{-5}$  M, (3)  $5 \times 10^{-5}$  M, (4)  $1 \times 10^{-4}$  M, (5)  $5 \times 10^{-4}$  M, (6)  $1 \times 10^{-3}$  M and (7)  $5 \times 10^{-3}$  M

The impedance spectra of the different Nyquist plots (Figures 1-3) were analyzed by fitting the experimental data to a simple equivalent circuit model, which includes the solution resistance  $R_s$  and the double layer capacitance  $C_{dl}$  which is placed in parallel to the charge transfer resistance  $R_{ct}$  (22). The  $R_{ct}$  values were calculated from the difference in impedance at low and high frequencies. The value of  $R_{ct}$  is a measure of electron transfer across the surface and inversely proportional to the corrosion rate. The double layer capacitance,  $C_{dl}$  were calculated at the frequency  $f_{max}$  at which the imaginary component of the impedance is maximal by the following equation

$$C_{dl} = \frac{1}{2\pi f_{max} R_{ct}} \quad (5)$$

The values of  $R_{ct}$ ,  $C_{dl}$  and %IE for C-steel in 2M hydrochloric acid containing different concentrations for the used inhibitors are shown in Tables (1-3). The data indicate that increasing charge transfer resistance is associated with a decrease in the double layer capacitance and increase in the percentage inhibition efficiency. The decrease in  $C_{dl}$  values could be attributed to the adsorption of the inhibitor molecules at the metal surface. It has been reported that the adsorption of organic inhibitor on the metal surface is characterized by a decrease in  $C_{dl}$  (25). Furthermore the decreased values of  $C_{dl}$  may be due to the replacement of water molecules at the electrode interface by organic inhibitor of lower dielectric constant through adsorption.

**Table 1.** Data obtained from EIS measurements for C-steel in 2M HCl in presence of different concentrations of inhibitor I.

Concentration (M)	$R_{ct}$ ( $\Omega\text{cm}^2$ )	$C_{dl}$ ( $\mu\text{F cm}^{-2}$ )	%IE	$\theta$
0.0	68.01	233.9	0.0	0.0
$5 \times 10^{-5}$	117.90	122.0	42.30	0.42
$1 \times 10^{-4}$	150.0	96.40	54.70	0.55
$5 \times 10^{-4}$	175.0	82.60	61.14	0.61
$1 \times 10^{-3}$	195.0	74.20	65.13	0.65
$5 \times 10^{-3}$	240.0	60.3	71.2	0.71

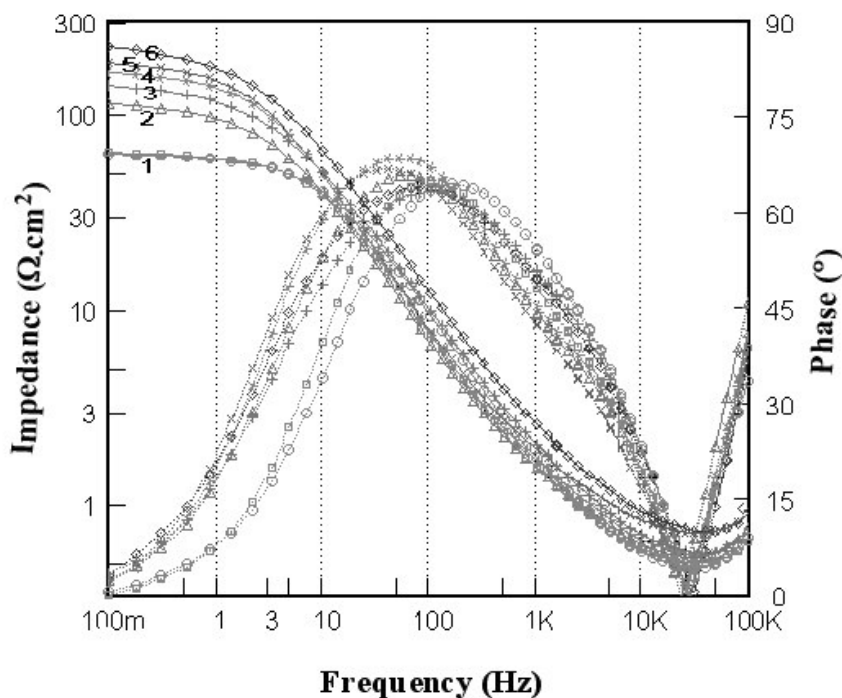
**Table 2.** Data obtained from EIS measurements for C-steel in 2M HCl in presence of different concentrations of inhibitor II.

Concentration (M)	$R_{ct}$ ( $\Omega\text{cm}^2$ )	$C_{dl}$ ( $\mu\text{F cm}^{-2}$ )	%IE	$\theta$
0.0	68.01	233.9	0.0	0.0
$5 \times 10^{-5}$	125.03	116.0	45.60	0.46
$1 \times 10^{-4}$	155.00	93.3	56.70	0.57
$5 \times 10^{-5}$	204.90	70.60	66.8	0.67
$1 \times 10^{-3}$	275.03	21.40	89.93	0.90
$5 \times 10^{-3}$	935.30	15.00	92.73	0.93

**Table 3.** Data obtained from EIS measurements for C-steel in 2M HCl in presence of different concentrations of inhibitor III.

Concentration (M)	$R_{ct}$ ( $\Omega\text{cm}^2$ )	$C_{dl}$ ( $\mu\text{F cm}^{-2}$ )	%IE	$\theta$
0.0	68.01	233.90	0.0	0.0
$5 \times 10^{-5}$	101.90	144.88	33.26	0.33
$1 \times 10^{-4}$	145.87	99.70	53.53	0.54
$5 \times 10^{-3}$	200.90	72.09	66.16	0.66
$1 \times 10^{-3}$	225.40	64.08	69.83	0.70
$5 \times 10^{-3}$	250.80	57.90	72.90	0.73

Bode plots for effect of pyrimidine derivatives on the corrosion of C-steel in 2MHCl solution are shown in Figures (4-6). The high frequency limit corresponds to the solution resistance  $R_s$ , while the lower frequency limit represents the summation of  $R_s+R_{ct}$ . Values of  $R_{ct}$ ,  $C_{dl}$  and %IE calculated from Nyquist and Bode plots are in good agreement. For Bode plots at both high and low frequency limits, the phase angle between current and potential,  $\theta^\circ$ , in all cases assume a value of  $0^\circ$ , corresponding to resistive behavior of  $R_s$  and  $R_s+R_{ct}$ . The dielectric properties of the adsorbed film are evident at intermediate frequencies as indicated by the capacitive behavior of the system. The presence of one phase maximum at intermediate frequencies indicates the presence of one time constant corresponding to the impedance of the formed protective film. In Bode plots for pure capacitive behavior the slope of log impedance vs. log frequency relation should be -1.

**Figure 4.** Bode plots of C-steel in 2M HCl in presence of different concentrations of inhibitor I at 25 °C. (1) blank, (2)  $5 \times 10^{-5}$  M, (3)  $1 \times 10^{-4}$  M, (4)  $5 \times 10^{-4}$  M, (5)  $1 \times 10^{-3}$  M and (6)  $5 \times 10^{-3}$  M

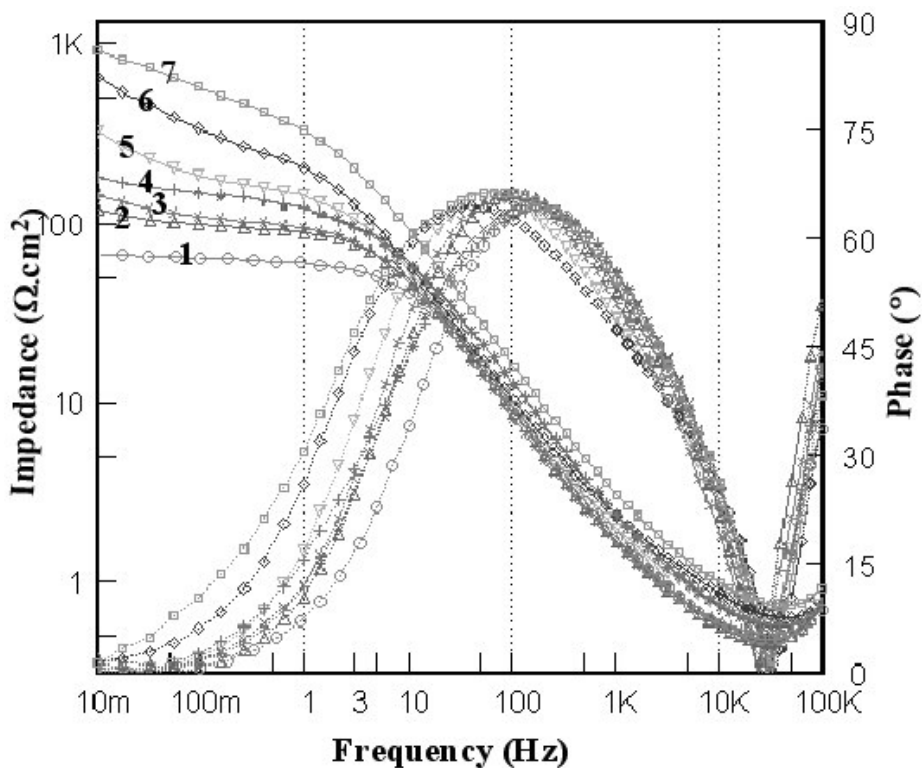


**Figure 5.** Bode plots of C-steel in 2M HCl in presence of different concentrations of inhibitor II at 25 °C. (1) blank, (2)  $1 \times 10^{-5}$  M, (3)  $5 \times 10^{-5}$  M, (4)  $1 \times 10^{-4}$  M, (5)  $5 \times 10^{-4}$  M, (6)  $1 \times 10^{-3}$  M and (7)  $5 \times 10^{-3}$  M

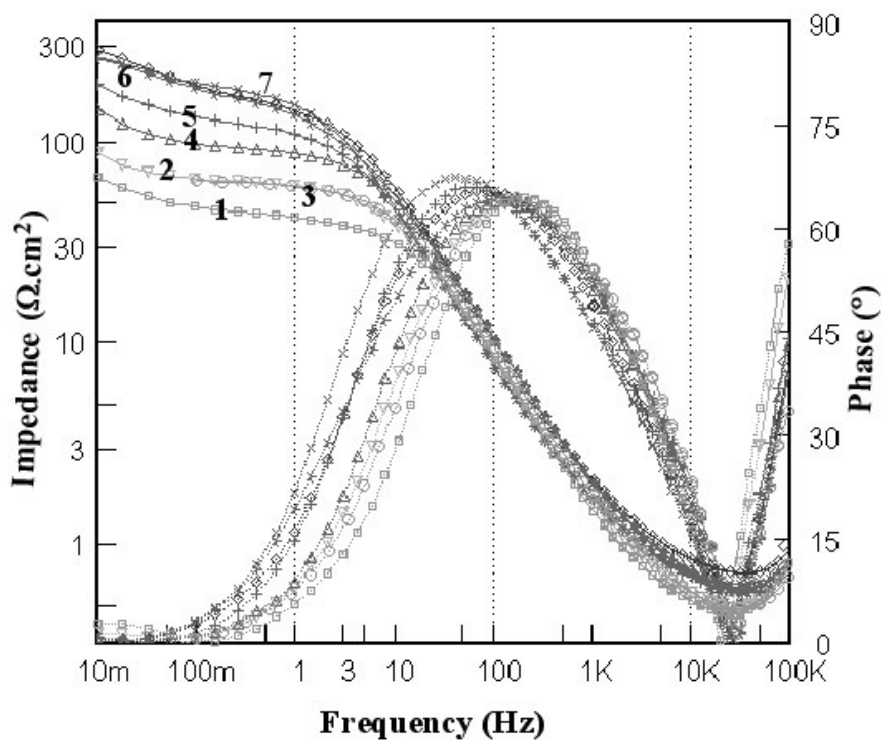


**Figure 6.** Bode plots of C-steel in 2M HCl in presence of different concentrations of inhibitor III at 25 °C. (1) blank, (2)  $1 \times 10^{-5}$  M, (3)  $5 \times 10^{-5}$  M, (4)  $1 \times 10^{-4}$  M, (5)  $5 \times 10^{-4}$  M, (6)  $1 \times 10^{-3}$  M and (7)  $5 \times 10^{-3}$  M



In the present work, most values of slopes were between -0.8 and -0.9, which indicate a capacitive behavior of the C-steel electrode under the experimental conditions. From the A.C. impedance technique data, at most inhibitor concentrations, the order of inhibition efficiency for the pyrimidine compounds is

$$\text{II} > \text{III} > \text{I}$$

### 3.2. Application of adsorption isotherm

Assuming a direct relationship between inhibition efficiency and the degree of surface coverage,  $\theta$ , for different concentrations of the inhibitor. Data obtained from EIS measurements were tested graphically for fitting various adsorption isotherms including Langmuir, Frunkin, Temkin and Frundich. By far the best fit was obtained with the Langmuir adsorption isotherm for the different inhibitors under investigation. According to this isotherm  $\theta$  is related to the inhibitor concentration  $C$  via

$$\frac{C}{\theta} = \frac{1}{K} + C \quad (6)$$

where  $K$  is the equilibrium constant.

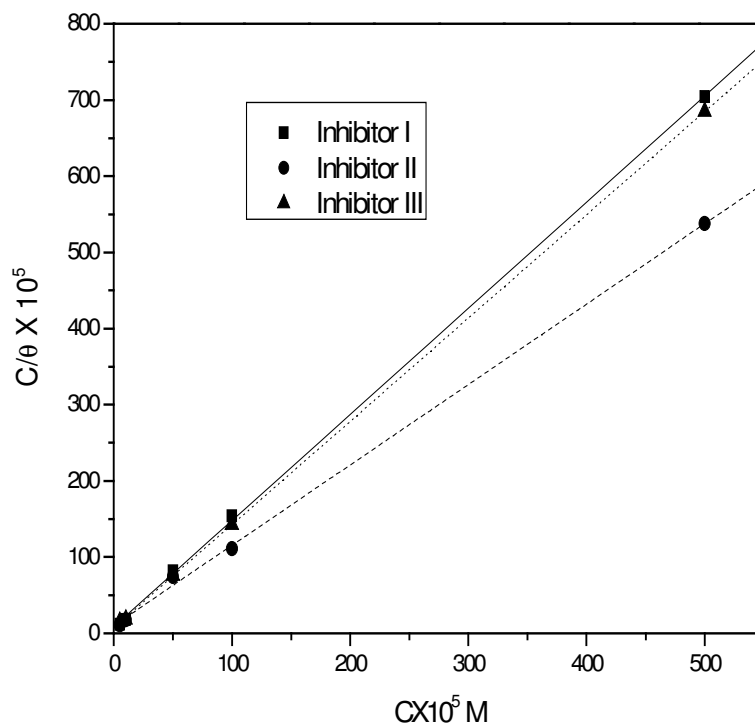


**Figure 7.** Langmuir adsorption isotherm plot for the adsorption of the used inhibitors, data obtained from EIS .

By plotting  $C/\theta$  vs.  $C$  a straight lines were obtained as shown in Figure 7. For inhibitor II, the slope of the straight line equals 1.05 which is close to unity indicating no interaction of the adsorbed molecules. For inhibitors I and III the slope of the straight lines deviate slightly from unity indicating the presence of mutual repulsion or attraction between the adsorbed molecules. Similar behavior was obtained for the adsorption of some organic inhibitors on iron surface in acid solutions (26-28). The intercept of the straight line permit the calculation of the equilibrium constant  $K$ , which leads to evaluate the standard free energy of adsorption  $\Delta G_{ads}^o$  from the following equation

$$K = \frac{1}{55.5} \exp^{\Delta G_{ads}^o / RT} \quad (7)$$

where  $R$  is the universal gas constant and  $T$  is the absolute temperature.

The calculated values of  $K$  and  $\Delta G_{ads}^o$  for inhibitor II amount to  $9.8 \times 10^3 \text{ mol}^{-1}$  and  $-32.68 \text{ KJ mol}^{-1}$  respectively. According to Donahue and Nobe (29), the value of  $\Delta G_{ads}^o$  indicates that inhibitor interacts on the C-steel surface by electrostatic effect. Also the negative value of  $\Delta G_{ads}^o$  points to the spontaneity of the adsorption process under investigated experimental conditions.

### 3.3. Weight-loss measurements

Weight-loss of C-steel at various time intervals, in the absence and presence of different concentrations of pyrimidine derivatives at  $25^\circ\text{C}$  was studied. The values of the corrosion rate ( $\text{mg}/\text{cm}^2 \cdot \text{min}$ ) and the percentage inhibition efficiency are presented in Table 4. It is clear that the decreasing corrosion rate is associated by increase in the %IE. Figure 8 shows the variation of the %IE with the concentration of the additives. The curves obtained indicate that the %IE increases with increasing the concentration of the additives.

**Table 4.** Data obtained from weight loss measurements for C-steel in 2M HCl in presence of different concentrations of the used inhibitors.

Concentration (M)	Rate of corrosion $\text{mg} \cdot \text{cm}^{-2} \cdot \text{min}^{-1}$			%IE		
	I	II	III	I	II	III
0.0	0.0310	0.031	0.031	0.0	0.0	0.0
$5 \times 10^{-5}$	0.0180	0.0167	0.0179	41.90	46.10	42.21
$1 \times 10^{-4}$	0.0143	0.0131	0.0139	53.92	57.81	55.81
$5 \times 10^{-3}$	0.0118	0.0101	0.0104	61.83	67.31	66.34
$1 \times 10^{-3}$	0.0108	0.00310	0.0091	64.92	90.10	70.54
$5 \times 10^{-3}$	0.0091	0.0021	0.0083	70.60	93.32	73.38

From the weight loss measurements the order of inhibition efficiency for the used inhibitors is  $\text{II} > \text{III} > \text{I}$  which is in good agreement with those obtained from EIS technique.

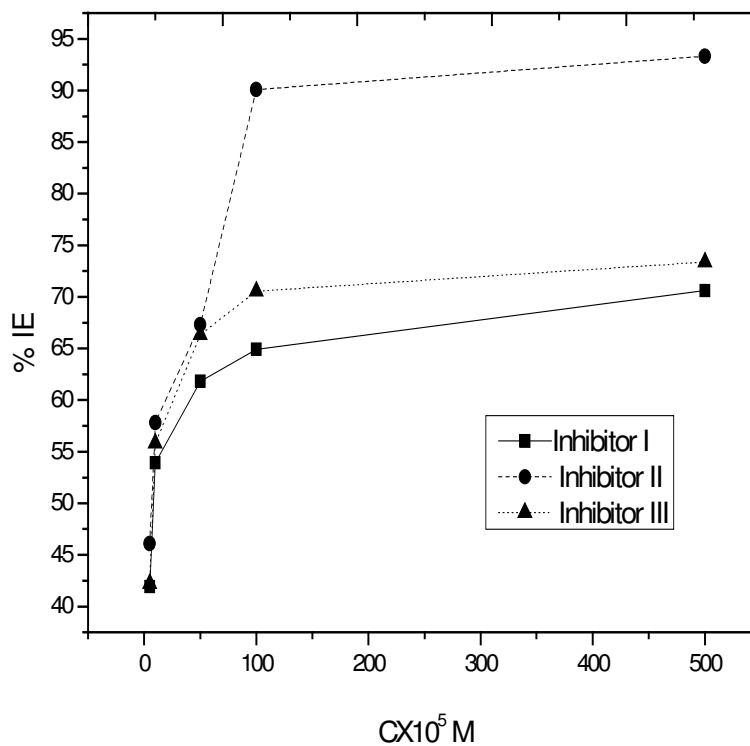


**Figure 8.** Effect of concentration of pyrimidine derivatives on %IE , data obtained from weight loss.

### 3.4. Mechanism of inhibition and molecular structure

As far as the inhibition process is concerned, it is generally assumed that the adsorption of the inhibitors at the metal solution interface is the first step in the action mechanism of inhibitors in aggressive acid media. Inhibition of C-steel in HCl solution by the pyrimidine derivatives can be explained on the basis of adsorption. Four types of adsorption may take place involving organic molecules at the metal solution interface (i) electrostatic attraction between charged molecules and the charged metal, (ii) interaction of  $\pi$ -electrons with the metal, (iii) interaction of uncharged electron pairs in the molecule with the metal and (iv) a combination of the above (20). It is apparent that the adsorption of these pyrimidine compounds on the Fe surface could occur directly on the basis of donor acceptor between the lone pairs of the heteroatoms and the extensively delocalized  $\pi$ -electrons of the pyrimidine molecule and the vacant d-orbitals of iron surface atoms (30). Moreover the presence of the electron releasing two methyl groups in the molecules increase the electron density on the pyrimidine heterocyclic ring.

In acidic solution, these compounds can exist as protonated species. These protonated species may adsorb on the cathodic sites of C-steel surface and decrease the evolution of hydrogen. These compounds are able to adsorb on anodic sites through N atoms, azomethine group, heterocyclic and aromatic rings which are electron donating groups. The adsorption of these compounds on anodic sites may decrease anodic dissolution of C-steel.

Inhibition effect of different compounds used in this investigation was observed from two different techniques and the order of inhibition efficiency is II > III > I. The effectiveness of a

compound as corrosion inhibitor mainly depends on the size and the active centers of the compound. The improved performance of inhibitor II and III over compound I can be attributed to the smallest size of this compound. The best performance of compound II as corrosion inhibitor over compound III may be attributed to the presence of OH and NO<sub>2</sub> groups in compound III. The electrophilic (electron withdrawing) character of NO<sub>2</sub> group is highest than the nucleophilic (electron releasing) character of OH group which hinders the delocalized  $\pi$ -electrons on the aromatic ring. On the other hand, the lower inhibition efficiency of the nitro derivative compound as compared to compound II may be due to its reduction in acid medium and the evolved heat of hydrogenation may aid the desorption of the molecules.

Moreover, the results obtained from the relation between inhibition characteristics and quantum chemical data show that %IE mostly depends upon the energies of the highest occupied molecular orbital (HOMO) and the lowest unoccupied molecular orbital (LUMO). Table 5 includes HOMO and LUMO values for compounds II and III. From this table it is evident that the inhibition efficiency increases with the increase of the ionization potential. It is further evident that the inhibition efficiency increases with the ease of ionization of the molecule, which means that the molecule acts as an electron donor when blocking the corrosion reaction.

**Table 5.** HOMO and LUMO values of compounds II and III.

Inhibitor	%IE in presence of $5 \times 10^{-3} \text{M}$	HOMO eV	LUMO eV
II	93.30	-9.456	-0.256
III	73.40	-9.661	-1.191

#### 4. CONCLUSIONS

All the examined pyrimidine derivatives are effective corrosion inhibitors for C-steel in 2M HCl solution.

The N-benzylidene-4,6-dimethylpyrimidine-2-amine gives the highest inhibition efficiency.

The investigated compounds inhibit corrosion by adsorption mechanism.

The adsorption of these compounds on the C-steel surface was found to obey Langmuir adsorption isotherm.

The order of the inhibition efficiency of inhibitors as given by EIS measurements is in good agreement with that obtained from weight loss measurements.

#### References

1. K.E. Heuslor and G.H. Cartledge, *J. Electrochem. Soc.*, 108 (1961) 732.
2. G. Tarbanelli, F.zucchi and G.L. Zucchini, *Corrosion Traitment, Protection, Finition*, 16 (1968) 335.
3. R.R. Armand, R.M. Hurd and N. Hackerman, *J. Electrochem. Soc.*, 112 (1965) 138.

4. G. Perboni and G. Rocchini, 10<sup>th</sup> ICMC, Madras, India, (1988) 193.
5. F. Zucchi and G. Tarbanelli, Proc. of the 7ESIC, Ann. Univ. Ferrara, Italy, Scz, Suppl., 9 (1990) 339.
6. B.G. Ateya, B.E. El-Anadoli and F.M. El-Nizamy, *Corros. Sci.*, 24 (1984) 497.
7. S. Muralidharan, K.L.N. Phari, S. Pitchuman, S.Rovic Harden and S.V.K. Ayer, *J. Electrochem. Soc.*, 142 (1995) 1478.
8. S. Syed Azim, S. Muralidharan, and S.V.K. Iyer, *J. Appl. Electrochem.*, 25 (1995) 495.
9. S. Murlidharan, B. Ramesh Bahu, S. Venkatakrishna and S. Rengmani, *J. Appl. Electrochem.*, 26 (1996) 291.
10. M. Th. Makhlof, S.A. El-Shatory and A. El-Said, *Mater. Chem. Phys.*, 43 (1996) 76.
11. P. Li, J.Y. Lin, K.L. Tan and J.Y. Lee, *Electrochim. Acta*, 42 (1997) 605.
12. A. Agrawal and T.K.G. Numboodhiri, *J. Appl. Electrochem.*, 23 (11) (1997) 1265.
13. S.S. Abd El-Rehim, M.A.M. Ibrahim and K.F. Khaled, *Corros. Prevent. Control*, 46(6) (1999) 157.
14. Y. Feug, K.S. Siow, W.K. Teb and A.K. Hsieh, *Corros. Sci.*, 41 (1999) 829.
15. L. El Kadi, B. Memari, M. Traisnel, F. Bentiss and M. Lagrenee, *Corros. Sci.*, 42 (2000) 703.
16. M.S. Morad, *Corros. Sci.*, 42 (2000) 1307.
17. M. Gajic, *Corros. Sci.*, 43 (2001) 919.
18. S. Martinez, *J. Appl. Electrochem.*, 31(9) (2001) 973.
19. M.A. Ameer, E. Khamis and G. Al-Senani, *J. Appl. Electrochem.*, 32(2) (2002) 149.
20. D. Schweinsberg, G. George, A. Nanayakkawa and D. Steinert, *Corros. Sci.*, 28 (1988) 33.
21. K.F. Bonhoeffer and K.E. Heascer, *Z. Phys. Chem.*, NE8 (1956) 390.
22. D.D. Macdoald, *Transient Techniques in Electrochemistry*, Plenum Press, New York (1977).
23. X. Yang, P. Xu, Q. Gao and M. Tan, *Synth. React. Inorg. Met.-Org. Chem.*, 32 (2002) 59.
24. K. Jutner, *Electrochim. Acta*, 35(10) (1990) 1501.
25. K. Aramaki, M. Hagiwara and H. Nishihara, *Corros. Sci.*, 5 (1987) 487.
26. A.K. Shams El-Din and J.M. Abd El-Kader, *Oberflachel Surface*, 18 (1977) 11.
27. A.A. Abdul Azim, L.A. Shalapy and H. Abbas, *Corros. Sci.*, 14 (1997) 1286.
28. A.K. Mohamed, A.A. El-Shafei, A.M. Abo-El-Wafa and Y.A. El-Ewady, *Bulletin of Electrochemistry*, 17 (2001) 145.
29. F.M. Donahue and K. Nobe, *J. Electrochem. Soc.*, 112 (1965) 886.
30. S. Muralidharan, M.A. Quraishi and S.V.K. Iyer, *Corros. Sci.*, 37 (1995) 1739.